Journal of Zhejiang University-SCIENCE A (Applied Physics & Engineering) 2025 26(2):138-150
www.jzus.zju.edu.cn; www.springer.com/journal/11582
E-mail: jzus_a@zju.edu.cn

Research Article
https://doi.org/10.1631/jzus.A2400040

Parameter matching and optimization of hybrid excavator swing system

Chao SHEN[1,2], Jianxin ZHU[1,2✉], Jian CHEN[1], Saibai LI[2], Lixin YI[1,2]

[1]State Key Laboratory of Precision Manufacturing for Extreme Service Performance, Central South University, Changsha 410083, China
[2]The National Enterprise R&D Center, Sunward Intelligence Equipment Co., Ltd., Changsha 410100, China

Abstract: In this study, a novel synergistic swing energy-regenerative hybrid system (SSEHS) for excavators with a large inertia slewing platform is constructed. With the SSEHS, the pressure boosting and output energy synergy of multiple energy sources can be realized, while the swing braking energy can be recovered and used by means of hydraulic energy. Additionally, considering the system constraints and comprehensive optimization conditions of energy efficiency and dynamic characteristics, an improved multi-objective particle swarm optimization (IMOPSO) combined with an adaptive grid is proposed for parameter optimization of the SSEHS. Meanwhile, a parameter rule-based control strategy is designed, which can switch to a reasonable working mode according to the real-time state. Finally, a physical prototype of a 50-t excavator and its AMESim model is established. The semi-simulation and semi-experiment results demonstrate that compared with a conventional swing system, energy consumption under the 90° rotation condition could be reduced by about 51.4% in the SSEHS before parameter optimization, while the energy-saving efficiency is improved by another 13.2% after parameter optimization. This confirms the effectiveness of the SSEHS and the IMOPSO parameter optimization method proposed in this paper. The IMOPSO algorithm is universal and can be used for parameter matching and optimization of hybrid power systems.

Key words: Hybrid system; Energy regeneration; Swing braking energy; Parameter optimization; Improved multi-objective particle swarm optimization (IMOPSO); Adaptive grid

1 Introduction

Excavators are one of the most common forms of machinery in the construction and mining industries. More than 95% of excavators in use are hydraulic excavators. However, conventional hydraulic excavators suffer from the problems of high energy consumption, low energy utilization, and poor emissions (Haga et al., 2001; Gong et al., 2020). Increasing environmental pollution and energy costs promote the development of novel energy-saving technology for hydraulic excavators (Tong et al., 2020).

In recent years, research on the energy recovery of excavators has focused mainly on the gravity potential energy recovery of boom working devices. In contrast, less research has been conducted on swing braking energy regeneration systems in complex working conditions (Lin et al., 2017; Do et al., 2021; Qu et al., 2021). At present, the energy regeneration schemes of swing systems can be summarized into two types, the pure electric scheme (Abdel-baqi et al., 2015; Tong et al., 2021) and the hybrid system scheme (Thompson et al., 2014; Wang et al., 2017; Tong et al., 2020). Pure electric schemes are used mainly for small- and medium-sized pure electric engineering machinery as they are affected by the endurance and output power of electric energy storage units and motors. Hybrid systems have wider applicability and reliability. Fuel-electric hybrid and fuel-hydraulic hybrid are common hybrid schemes. Many scholars have carried out modeling and experimental research on fuel-electric hybrid systems, achieving the regeneration of swing energy (Kwon et al., 2010; Lin et al., 2014; Liu et al., 2016; Gong et al., 2019b). Nevertheless, the limited space of the excavator, as well as the high additional costs caused by the use of supercapacitors and other components makes fuel-electric hybrid schemes not the optimal choice at present (Latas and Stojek, 2018).

✉ Jianxin ZHU, zjianx-918@163.com
Chao SHEN, https://orcid.org/0000-0002-6950-4149
Jianxin ZHU, https://orcid.org/0000-0001-7577-2070

Received Jan. 21, 2024; Revision accepted May 11, 2024; Crosschecked Dec. 27, 2024; Online first Jan. 21, 2025

Compared with fuel-electric hybrid systems, fuel-hydraulic hybrid systems are widely used due to their high compatibility, high power density, and low cost (Xia et al., 2018). Ho and Ahn (2012) proposed a fuel-hydraulic swing system with a closed-loop transmission structure. Based on the premise of not reversing fluid flow, the swing energy is regenerated through a four-quadrant pump/motor, achieving an energy recovery rate of between 22% and 59%. Lin et al. (2013) constructed a swing energy-saving system combining hydraulic energy storage and a pump control system, in which the braking energy is converted and stored in the accumulator and timely released to drive the main pump to rotate. Caterpillar has released multiple patents for energy-saving rotary systems using hydraulic excavators, with the use of control valves and hydraulic accumulators to recover and reuse the swing braking energy (Shang et al., 2014; Hillman et al., 2016). Yu and Ahn (2020a; 2020b) established a novel fuel-hydraulic excavator swing energy-saving system with a variable motor and a valve-controlled accumulator. However, the presence of a flow-proportional valve leading to throttling loss weakens the energy-saving performance of the system.

A reasonable system structure and control strategy are key factors in the design of swing hybrid systems, while appropriate parameter matching is also crucial for improving the energy-saving performance of such systems (Lin and Liu, 2013). The model-based parameter optimization and matching method can significantly shorten the design cycle and obtain a better parameter combination (Borthakur and Subramanian, 2019; Gong et al., 2019a). However, it is challenging to obtain the optimal combination of control parameters due to parameter coupling. Model-based intelligent optimization algorithms are an effective method to address this issue. Common intelligent optimization algorithms include the particle swarm optimization (PSO) algorithm (Poli et al., 2007; Wang and Wang, 2020), genetic algorithm (GA) (Chen et al., 2018), and simulated annealing (SA) algorithm (Suppapitnarm et al., 2000). PSO has gained widespread application for system parameter matching and optimization due to its simplistic structure, rapid convergence speed, and exceptional global search capability (Clerc and Kennedy, 2002; Prasanthi et al., 2021; Wei et al., 2022). Nevertheless, according to current research, there have been few investigations of parameter matching and optimization of excavator hybrid systems based on intelligent algorithms, and minimal research has been conducted on the multi-objective parameter optimization of key components in swing hybrid systems.

Given the significant energy-saving benefits of swing braking energy regeneration, a novel synergistic swing energy-regenerative hybrid system (SSEHS) for excavators with large-inertia slewing platforms was developed in this study. In this system, the swing braking energy of the excavator is efficiently recovered and reused. Unlike conventional parameter matching methods for hybrid systems, an improved multi-objective particle swarm optimization (IMOPSO) algorithm is proposed to optimize the system's key parameters, including displacement of the hydraulic transformer (HT) and the volume and pressure of the accumulator.

2 System configuration

A slewing platform with a large inertia of the hydraulic excavator frequently performs rotary acceleration-braking motion during the working process. In this section, the working principle and energy loss mechanism of the conventional swing system of a hydraulic excavator are analyzed, and a novel swing energy-saving system is presented.

2.1 Conventional swing system

Fig. 1 shows the structure of two types of excavator swing systems. Fig. 1a shows a conventional swing system composed of a pilot handle control system, hydraulic pump, swing motor, swing mechanism, and valve-control devices.

There are four motion states of a slewing platform: stationary, accelerated swing, uniform swing, and braking. During the working motion, a lot of energy is lost due to the working characteristics of the swing hydraulic system. This results in excessive energy consumption, a low energy utilization rate, and poor exhaust emissions. Based on current research, the energy loss of a swing system comes mainly from four sources: the acceleration overflow loss and the brake overflow loss in the relief valve, the throttle loss in the main valve, and the mechanical loss in the swing mechanism. Among these, the mechanical loss cannot be avoided, while the overflow energy loss can be reduced by means of energy regeneration and flow matching.

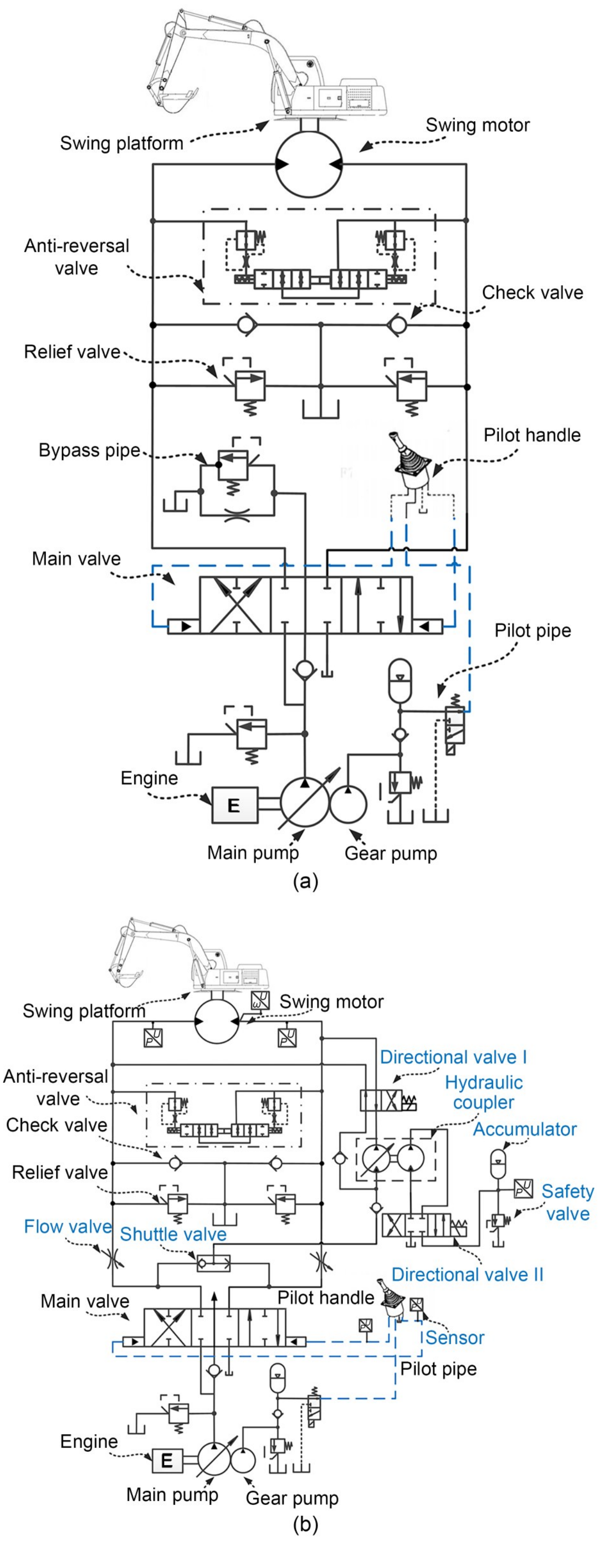

Fig. 1 Swing systems of excavators: (a) conventional swing system; (b) SSEHS

2.2 Synergistic swing energy-regenerative hybrid system (SSEHS)

To reduce the energy consumption of a swing system with a large-inertia slewing platform, we propose the SSEHS (Fig. 1b). The SSEHS is composed mainly of an HT, hydraulic energy storage unit, pilot handle control system, hydraulic pump, and some necessary control valves. In the hydraulic energy storage unit, the hydraulic accumulator serves as an energy storage element to store the recovered swing energy. The HT used in this system is composed of a variable displacement pump/motor and a fixed displacement pump/motor connected by a rigid shaft, which inherits the characteristics of high efficiency and high reliability of the hydraulics/motor.

During the SSEHS working process, the proposed system has three working states: energy release, energy recovery, and stationary. Each working state is elaborated as follows:

(1) Energy release state. The main pump outputs energy and drives the left hydraulic pump/motor of the HT to rotate through the main valve and shuttle valve, while the left hydraulic pump/motor of the HT is driven by the output energy from the accumulator. As a result, the swing motor and slewing platform begin to rotate under the synergistic work of the two energy sources. To reduce the overflow loss during acceleration, the pressure on both sides of the swing motor is measured in real time and fed back to the controller. Then, the displacement of the main pump is adjusted by the controller, and the output energy of the main pump is reasonably matched.

(2) Energy recovery state. When the slewing platform is in the braking process, the main valve and the right flow valve are closed. Immediately, the pressure on the right side of the swing motor rises rapidly. Then, the hydraulic oil on the right side of the swing motor flows into the HT through the directional valve I and the check valve, driving the HT to rotate continuously. Controlled by the HT, the braking energy of the slewing platform is recovered and stored in the hydraulic accumulator.

(3) Stationary state. When the swing energy recovery is completed, the directional valve II works in the neutral position. The hydraulic energy storage unit is closed. The main valve is in the neutral position, and the slewing platform is in a stationary state.

3 Parameter matching and optimization

Reasonable parameter matching can optimize the dynamic characteristics and improve the energy efficiency of the energy-saving system. Unlike the conventional parameter matching methods used in hybrid systems, in this section, an IMOPSO algorithm with an adaptive grid considering system constraints is established, and the optimization principles and processes are explained.

3.1 IMOPSO considering constraints

3.1.1 Fundamental principles and evaluation criterion

The issue of multi-objective optimization can usually be described as follows:

$$\begin{aligned}&\min F=[f_1(\boldsymbol{X}),f_2(\boldsymbol{X}),\cdots,f_m(\boldsymbol{X})]^{\mathrm{T}},\\&\boldsymbol{X}=[x_1,x_2,\cdots,x_M]^{\mathrm{T}},\ \boldsymbol{X}\in\mathbb{R}^M,\\&\text{s.t.}\begin{cases}g_\varphi(\boldsymbol{X})\leqslant 0, & \varphi=1,2,\cdots,p,\\ h_\psi(\boldsymbol{X})=0, & \psi=1,2,\cdots,q,\\ \lambda_i\leqslant x_i\leqslant\gamma_i, & i=1,2,\cdots,M,\end{cases}\end{aligned}\tag{1}$$

where m, M, p, and q are the number of objective functions, state variables, inequality constraints, and equality constraints, respectively. λ_i and γ_i are the boundary values of the ith state variable. $F(\boldsymbol{X})=[f_1(\boldsymbol{X}),f_2(\boldsymbol{X}),\cdots,f_m(\boldsymbol{X})]^{\mathrm{T}}$ is the m-dimensional objective function vector, and $g_\varphi(\boldsymbol{X})$ and $h_\psi(\boldsymbol{X})$ are the inequality constraint and equality constraint, respectively.

For the multi-objective optimization issue illustrated in Eq. (1), the velocity and position of particle $\boldsymbol{X}$ after the (k+1)th iteration of multi-objective particle swarm optimization (MOPSO) with m-dimensional decision variables can be calculated by the following equations:

$$\boldsymbol{X}^{(k+1)}=\boldsymbol{X}^{(k)}+\boldsymbol{V}^{(k+1)},\tag{2}$$

$$\begin{aligned}\boldsymbol{V}^{(k+1)}=\omega^{(k)}\boldsymbol{V}^{(k)}&+c_1r_1(\boldsymbol{P}_{\text{best}}^{(k)}-\boldsymbol{X}^{(k)})\\&+c_2r_2(\boldsymbol{G}_{\text{best}}^{(k)}-\boldsymbol{X}^{(k)}),\end{aligned}\tag{3}$$

where $\omega^{(k)}$ denotes the inertia coefficient which varies with the number of iterations, c_1 is the individual learning coefficient, c_2 is the social learning coefficient, and r_1 and r_2 are random values uniformly distributed within (0, 1). $\boldsymbol{P}_{\text{best}}^{(k)}$ denotes the individual best historical position of each particle after k iterations, and $\boldsymbol{G}_{\text{best}}^{(k)}$ denotes the global best historical position of the entire swarm.

Note that while a traditional PSO can solve a single-objective optimization problem without constraints, it cannot effectively solve a multi-objective optimization problem with system constraints. To address this issue, evaluation criteria are designed using the Patro dominance theory as follows:

(1) The particles that do not violate the constraints are superior to the particles that violate the constraints.

(2) If both particles violate the constraints, the particle with a smaller degree of constraint violation dominates.

(3) If both particles do not violate the constraints, the non-dominated particle is optimal based on the Pareto dominance theory.

In the above evaluation criteria, the degree of constraint violation of the particle is defined as

$$Q(\boldsymbol{X})=\sum_{\varphi=1}^{p}\frac{\max(0,\ g_\varphi(\boldsymbol{X}))}{G_\varphi(\boldsymbol{X})}+\sum_{\psi=1}^{q}\frac{\max\left(0,\ |h_\psi(\boldsymbol{X})|\right)}{H_\psi(\boldsymbol{X})},\tag{4}$$

where $G_\varphi(\boldsymbol{X})=\max\left(|g_\varphi(\boldsymbol{X}_1)|,|g_\varphi(\boldsymbol{X}_2)|,\cdots,|g_\varphi(\boldsymbol{X}_N)|\right)$ and $H_\psi(\boldsymbol{X})=\max\left(|h_\psi(\boldsymbol{X}_1)|,|h_\psi(\boldsymbol{X}_2)|,\cdots,|h_\psi(\boldsymbol{X}_N)|\right)$, in which N denotes the number of populations. For particles that satisfy the constraints, $Q(\boldsymbol{X})$=0. The larger the value of $Q(\boldsymbol{X})$, the farther the particle is from the feasible region.

3.1.2 Archive and adaptive grid

The Archive is a collection used to record the information of non-dominated particles in the optimization process of the IMOPSO algorithm. An adaptive grid construction method is used to obtain the Pareto optimal solution and improve the solution convergence and diversity of the IMOPSO. The m-dimensional objective space composed of m-objective functions is divided into $K_1\times K_2\times\cdots\times K_m$ hyperplane grids, and the modulus of the ith objective function of each grid is defined as

$$d_i=\frac{\max f_i(\boldsymbol{X})-\min f_i(\boldsymbol{X})}{K_i}.\tag{5}$$

Coding transformation is used to encode the grid of the particle, and the grid number of the ith particle can be obtained from:

$$N_{gi} = N_1 + K_1 N_2 + \cdots + K_{m-1} N_m, \tag{6}$$

where N_1, N_2, ⋯, N_m is the number of the ith particle in each grid. The particles are in the same grid while the grid numbers N_{gi} of different particles are equal. The lower the particle density value, the greater the probability of being selected as the global optimal particle and the smaller the probability of being deleted, so as to improve the diversity and global search ability, and avoid the premature phenomenon.

The calculation step flow of the IMOPSO algorithm with adaptive grid considering system constraints is illustrated in Fig. 2.

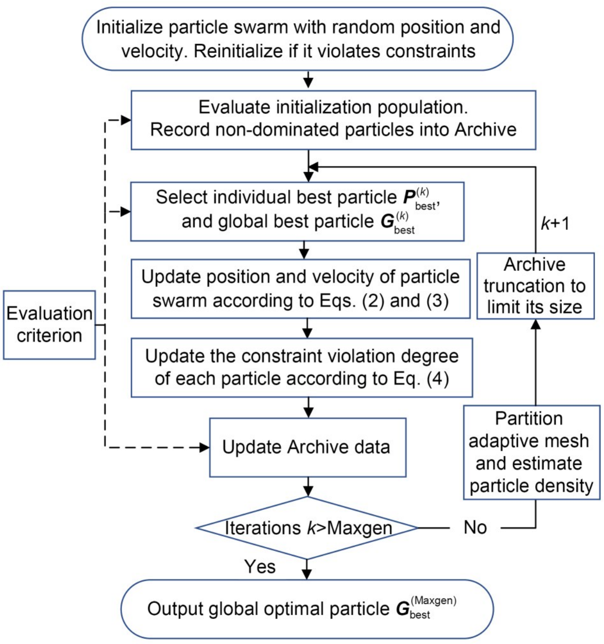

Fig. 2 Calculation step of the IMOPSO

3.2 Parameter optimization

Within the proposed SSEHS, the HT and accumulator are the key components that have a significant impact on the efficiency and dynamic characteristics. Therefore, in this section, the parameters of these two important components will be matched and optimized using the IMOPSO algorithm.

3.2.1 Parameter matching objective

A typical working cycle of an excavator can be divided into four stages: excavation, full-load rotation, unloading, and empty-load rotation, among which 90° rotation movement is the most common working condition. Therefore, this working condition was selected as the standard parameter matching condition, and the following parameter optimization objectives (1)–(3) were formulated:

(1) The input energy required by the main pump during the movement of the slewing platform is small, and the system has high energy-saving efficiency.

(2) The energy storage unit of the SSEHS has high energy storage efficiency.

(3) The energy stored and released by the energy storage unit is balanced after a working cycle.

3.2.2 Decision variable selection

The displacements of the HT motor/pump V_h, the pre-charge pressure P_0, and the corresponding gas volume of the accumulator V_0 are taken as the decision variables of the multi-objective optimization.

$$\boldsymbol{X} = [x_1, x_2, x_3, x_4]^\text{T} = [V_\text{hL}, V_\text{hR}, P_0, V_0]^\text{T}, \tag{7}$$

where V_hL denotes the displacement of the left HT motor/pump, and V_hR denotes the displacement of the right HT motor/pump.

3.2.3 Objective function design

According to Objective 1 set in Section 3.2.1, the energy-saving objective function $f_1(\boldsymbol{X})$ is designed as follows:

$$\begin{aligned} f_1(\boldsymbol{X}) &= E_\text{sin} - E_\text{acc} - E_\text{loss} \\ &= \frac{E_\text{sk}}{\eta_\text{sm}\eta_\text{sre}} - \frac{x_3^{\frac{1}{n}} x_4}{1-n}\left(P_1^{\frac{n-1}{n}} - P_2^{\frac{n-1}{n}}\right) \\ &\quad - \frac{2.5\times10^{-7}\left(1+\dfrac{\eta_\text{m}x_2}{x_1}\right)\bar{P}_\text{d}}{\delta\cdot x_1}\int Q_\text{m}\text{d}t \\ &\quad - \frac{8.1\times10^{-15}\left(1-\dfrac{\eta_\text{m}^2x_2^2}{x_1^2}\right)\bar{P}_\text{d}^2}{\delta\cdot x_1}\int Q_\text{m}\text{d}t \\ &\quad - \frac{5.84\times10^{-2}(\delta+1)}{2\pi\delta^2x_1^2}\int Q_\text{m}^2\text{d}t \\ &\quad - \frac{8.02\times10^{-4}(\delta^2+1)}{4\pi^2\delta^3x_1^3}\int Q_\text{m}^3\text{d}t. \end{aligned} \tag{8}$$

Here, the volume loss of HT is not considered. E_loss is the energy loss caused by the frictional torque, E_sk is the kinetic energy of the slewing platform, E_sin is the input energy of the swing motor, and E_acc is the energy stored or released when the pressure of the accumulator changes from P_1 to P_2, where P_1 is the limit of the minimum working pressure, and P_2 is the maximum working pressure. η_{sm} and η_{sre} are the total efficiency of the swing motor and the mechanical efficiency of the rotary reducer, respectively, and η_m is the total mechanical efficiency of the HT. n is the gas isotropic coefficient. P_d is the pressure in the inlet of the fixed displacement pump/motor. $\bar{P}_d$ represents the average value of P_d, δ is the displacement coefficient of the variable displacement pump/motor, and Q_m is the flow of the swing motor.

According to Objective 2, the objective function $f_2(\boldsymbol{X})$ of the energy density of the energy storage unit is designed as follows:

$$f_2(\boldsymbol{X})=-\frac{\mathrm{d}E_{acc}}{\mathrm{d}V_0}=-\frac{x_3^{\frac{1}{n}}}{1-n}\left(P_1^{\frac{n-1}{n}}-P_2^{\frac{n-1}{n}}\right). \tag{9}$$

According to Objective 3, the stability objective function $f_3(\boldsymbol{X})$ of the energy storage unit is designed as follows:

$$f_3(\boldsymbol{X})=-\frac{E_{sk}\eta_{rec}}{E_p+E_{acc}}= -\frac{E_{sk}\eta_{rec}}{\left(P_{a\_max}-\frac{\eta_m x_2\bar{P}_d}{x_1}\right)\int Q_m\mathrm{d}t+\frac{x_3^{\frac{1}{n}}x_4}{1-n}\left(P_1^{\frac{n-1}{n}}-P_2^{\frac{n-1}{n}}\right)}, \tag{10}$$

where E_p is the energy output by the hydraulic pump, P_{a_max} is the maximum pressure inside the connecting pipeline between the HT and the swing motor, and η_{rec} is the total efficiency of the swing motor and the rotary reducer.

Please refer to electronic supplementary materials (ESM) for the detailed modeling process.

3.2.4 Constraint determination

Based on a 50-t hydraulic excavator from SUNWARD company, some system parameters of the swing system are selected as: $\eta_{sm}=0.92$, η_{sre}=0.96, η_{rec}=0.88, η_m=0.91, E_{sk}=164.7 kJ, P_{a_max}=27 MPa, P_1= 20 MPa, P_2=30 MPa, n=1.4, V_m=130 mL, Q_{m_max}= 324 L/min, and $\eta_{hL}=\eta_{hR}$=0.93, where η_{hL} and η_{hR} are the efficiencies of the left motor/pump and right motor/pump of the HT, respectively. V_m is the displacement of the swing motor. Meanwhile, considering the limited installation space and the cost of components, the displacement of pumps/motors of the HT should be limited as:

$$55\leqslant V_{hL}\leqslant 200,\ 55\leqslant V_{hR}\leqslant 200. \tag{11}$$

To make the HT work in an efficient working state, its maximum output torque and speed should meet the following requirements:

$$\frac{P_{p\_max}\cdot V_{hL}}{2\pi}\cdot\eta_{hL}+\frac{P_2\cdot V_{hR}}{2\pi}\cdot\eta_{hR}\geqslant 2\cdot\frac{P_a\cdot V_m}{2\pi}\cdot\eta_m, \tag{12}$$

$$\frac{Q_{m\_max}}{V_{hL}}\leqslant 3000, \tag{13}$$

where P_{p_max} is the maximum output pressure of the main pump.

Additionally, to prolong the life of the energy storage unit, the limit of the minimum working pressure P_1, the initial working pressure P_0, and the maximum working pressure P_2 of the accumulator are limited as:

$$0.25P_2<P_0<0.9P_1,\ \lambda P_1<P_{a\_max}<\lambda P_2, \tag{14}$$

where λ is the transformer ratio of the HT.

Moreover, to improve the energy-saving efficiency of the system, the swing braking energy should be recovered as much as possible by the energy storage unit:

$$0.9E_{sk}\leqslant\frac{P_0^{\frac{1}{n}}V_0}{1-n}\left(P_1^{\frac{n-1}{n}}-P_2^{\frac{n-1}{n}}\right)\leqslant E_{sk}. \tag{15}$$

Based on the above analysis, the system constraints can be summarized as follows:

$$\begin{cases}55\leqslant x_1\leqslant 200,\\ 55\leqslant x_2\leqslant 200,\\ 0\leqslant x_3\leqslant 34,\\ 0\leqslant x_4\leqslant 200,\\ 0.25P_2<x_3<0.90P_1,\end{cases} \tag{16}$$

$$\begin{cases}g_1(\boldsymbol{X})=0.5P_{a\_max}x_1-P_1x_2,\\ g_2(\boldsymbol{X})=\frac{x_2}{x_1}P_2-P_{a\_max},\\ g_3(\boldsymbol{X})=236.6P_{a\_max}-0.93P_{p\_max}x_1-0.93P_2x_2,\\ g_4(\boldsymbol{X})=10^3\frac{Q_{m\_max}}{x_1}-3000,\\ g_5(\boldsymbol{X})=\frac{x_3^{\frac{1}{n}}x_4}{1-n}\left(P_1^{\frac{n-1}{n}}-P_2^{\frac{n-1}{n}}\right)-E_{sk},\\ g_6(\boldsymbol{X})=0.9E_{sk}-\frac{x_3^{\frac{1}{n}}x_4}{1-n}\left(P_1^{\frac{n-1}{n}}-P_2^{\frac{n-1}{n}}\right).\end{cases} \tag{17}$$

3.2.5 Optimization results

Selecting the maximum number of iterations as Maxgen=1000, the size of the Archive is n_{Arch}=100. The individual learning coefficient and the social learning coefficient are selected as $c_1=c_2=0.3$, while the maximum and minimum inertia weights are $\omega_{\max}$=1 and $\omega_{\min}$=0.1, respectively.

According to the calculation steps of the IMOPSO shown in Fig. 2, writing an optimization program in MATLAB, and performing three operations, the distribution of the optimization objective function obtained is illustrated in Fig. 3. Fig. 3a shows the distribution of the initial particle swarms, Fig. 3b shows the distributions of the optimized particle swarms after 1000 iterations, and Fig. 3c shows the particles in the Archive. From the optimization results, the initial particle swarm is randomly dispersed in the feasible region and converges after iteration. Note that a small number of particles diverge, which is due mainly to the characteristics of the adaptive grid division and the particle density evaluation shown in Eqs. (5) and (6). Particles with low density are more likely to be selected as the globally optimal particles, to improve the global search ability.

The particle ranges in the Archive are summarized in Table 1, where $\min F(\boldsymbol{X})=\min(f_1+f_2+f_3)$.

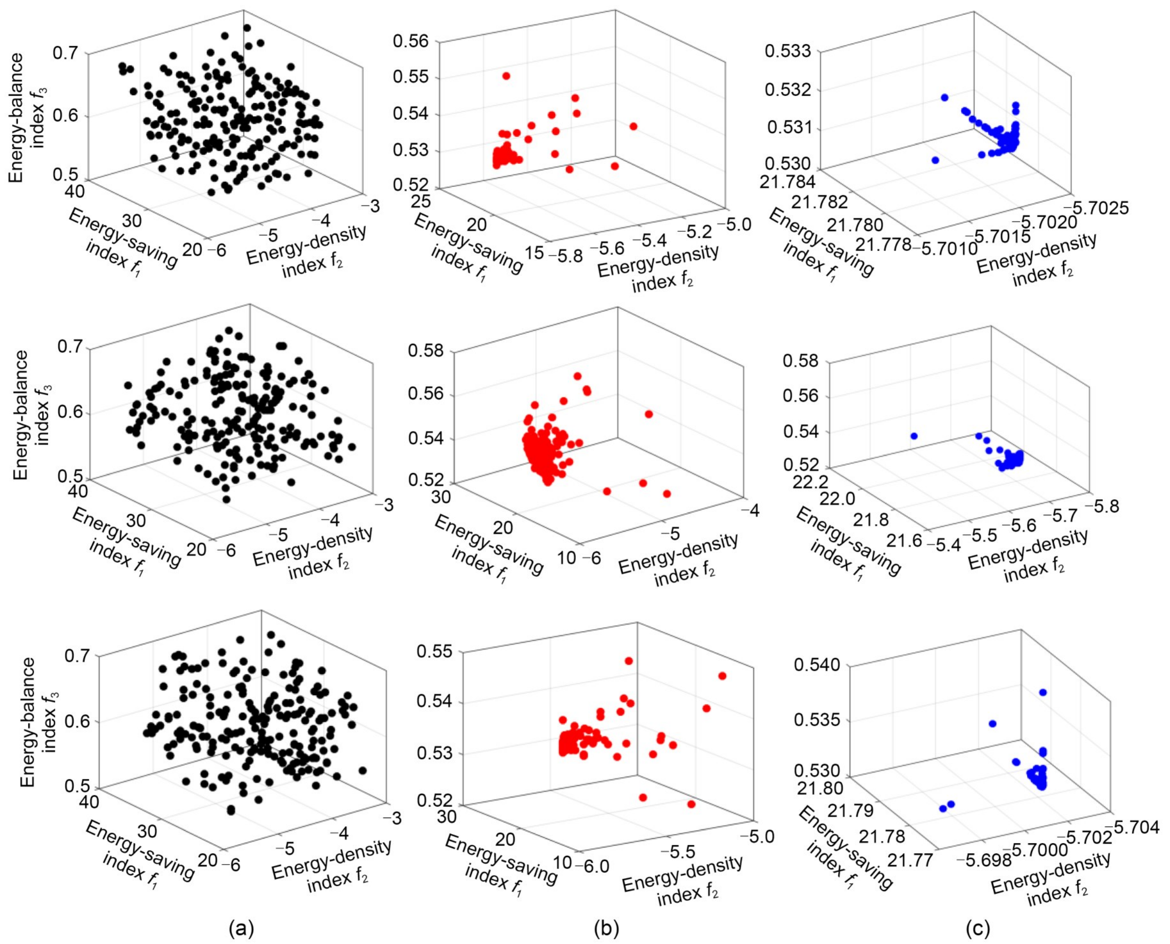

Fig. 3 Results of three-parameter optimization: (a) initial particle swarm; (b) optimized particle swarm; (c) particles in the Archive

Table 1 Ranges of particles in the Archive after optimization

Item	Left displacement of HT, V_{hL} (mL)	Right displacement of HT, V_{hR} (mL)	Pre-charge pressure, P_0 (MPa)	Gas volume, V_0 (L)
Minimum	170.8	114.4	17.9	28.2
Maximum	168.9	115.4	18.0	28.5
min$F$($\boldsymbol{X}$)	170.5	115.1	18.0	28.4

According to Table 1 and the existing variable pump/motor specifications, the system parameters are selected as V_{hL}=165 mL, V_{hR}=125 mL, P_0 = 18 MPa, and V_0 = 28 L.

4 Modeling and simulation

4.1 Model of the SSEHS

In this section, we describe the semi-simulation and semi-experiment research method applied to study the proposed energy-saving system. A 50-t hydraulic excavator prototype was established (Fig. 4). AMESim software is a kind of multidisciplinary platform dedicated to the modeling, simulation, and analysis of complex systems. With an extensive collection of model libraries and sophisticated modeling tools, AMESim can precisely emulate the intricate physical behaviors of complex systems, encompassing fluid dynamics, machinery, thermal fluids, and control systems. Based on the structure and parameters of the physical prototype, a simulation model was constructed

Fig. 4 The 50-t hydraulic excavator prototype

using AMESim (Fig. 5). To verify the accuracy of the constructed simulation model, the physical prototype and simulation model are compared under different swing angle conditions (45°, 90°, and 180°). In this process, the pilot control signal of the test prototype is collected and used as the input pilot signal of the simulation model. The results of the comparison are illustrated in Fig. 6.

Fig. 6 shows the results of a comparison of platform swing speed and pump pressure between the

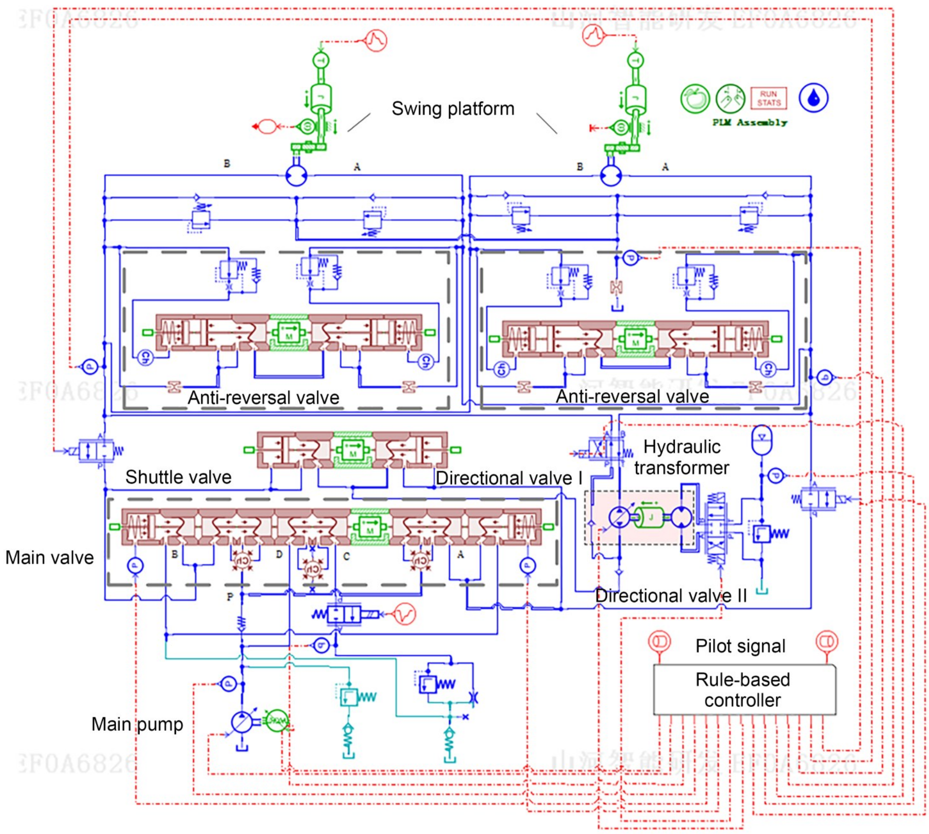

Fig. 5 Simulation model of the SSEHS

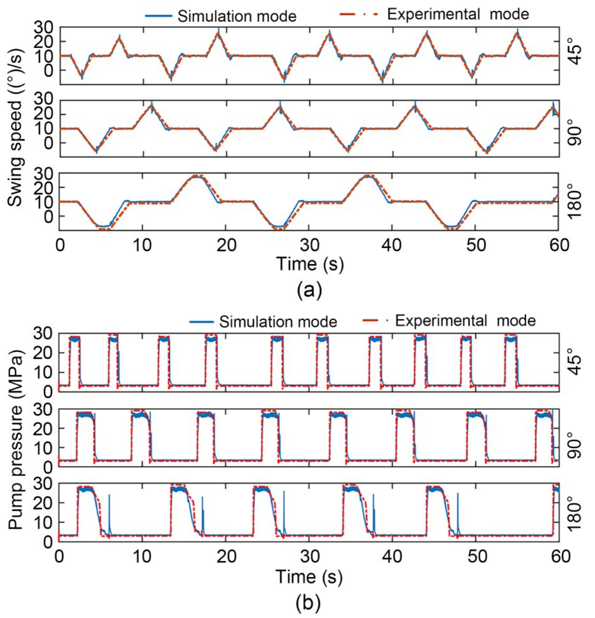

Fig. 6 Comparison of platform swing speed and pump pressure between the simulation model and the physical prototype under the same pilot signal control: (a) swing speed of slewing platform; (b) pump pressure

simulation model and the physical prototype under the same pilot signal control. By selecting reasonable system structure parameters, the working data of the simulation model in conventional mode and the measured data of the physical prototype were consistent in size and trend. This proves the rationality and accuracy of the constructed simulation model system. Meanwhile, it indicates that the energy-saving efficiency and dynamic characteristics of the SSEHS system can be further studied based on this simulation model. To further compare the effectiveness of the improved MOPSO algorithm proposed in this paper, a set of comparative parameters are designed using the conventional parameter selection methods: V_{hL}=180 mL, V_{hR}=90 mL, P_0=12 MPa, V_0=60 L, and P_2=30 MPa.

4.2 Rule-based control strategy design

The following feedback signals are selected to design the rule-based control strategy for the SSEHS: the pilot pressure signal P_j of the operating handle, the pressure P_m on both sides of the swing motor, the swing speed ω of the slewing platform, and the pressure P_X of the accumulator, in which P_{jL} and P_{jR} represent the left and right turn pilot pressure signals, respectively, and α and ω_c are constant values for the control. The rule-based control strategy designed is depicted in Fig. 7.

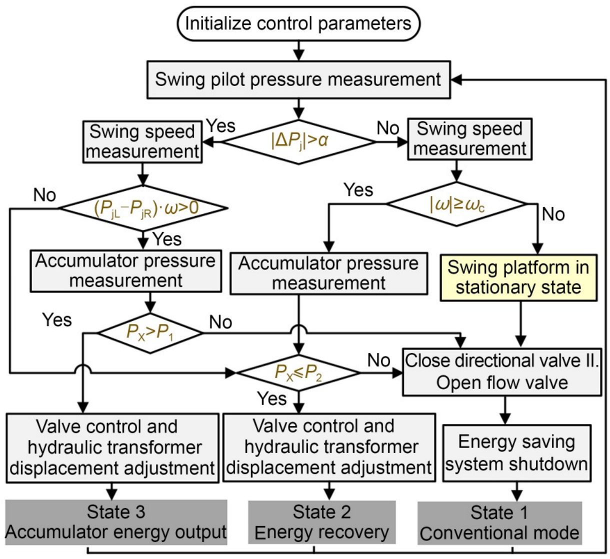

Fig. 7 Block diagram of the rule-based control strategy

The selection of control parameters directly affects the energy-saving efficiency and dynamic characteristics of the SSEHS. A large value of α results in a large pilot pressure required to start the slewing platform when the initial state of the slewing platform is stationary. Meanwhile, the value of ω_c determines the swing speed of the slewing platform when it ends the energy recovery state. The working pressures P_1 and P_2 of the hydraulic accumulator are the key parameters that affect the state switching of the SSEHS. Therefore, it is necessary to choose reasonable control parameters to obtain a better energy-saving rate under the premise of ensuring the slewing dynamics.

4.3 System dynamic analysis

In this subsection, we compare the system dynamic characteristics of three different swing systems: the swing system in the conventional mode, the SSEHS before parameter optimization, and the SSEHS after parameter optimization. Figs. 8 and 9 show the system dynamics of different swing systems.

Under the 90° swing condition, the maximum outlet pressure of the main pump in the conventional swing system is 27 MPa since the main pump is the only energy source. Compared with the conventional swing system, the outlet pressure of the main pump in the proposed SSEHS is greatly reduced due to the

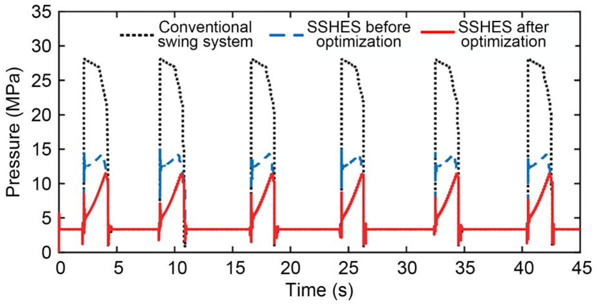

Fig. 8 Comparison of main pump outlet pressure of different systems

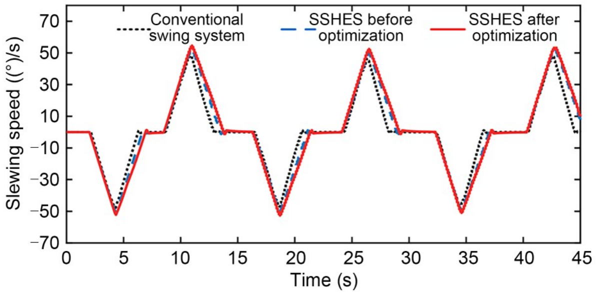

Fig. 9 Comparison of swing speeds of different systems

assistance of the auxiliary energy. Before parameter optimization, the maximum outlet pressure of the main pump in the SSEHS is 14.3 MPa, which reduces to 11.5 MPa after parameter optimization. Furthermore, in the stage of swing acceleration, the speed trend and size of the slewing platform of the three different systems are the same (Fig. 9), which proves that the proposed SSEHS can effectively reduce the output power of the main pump without affecting the swing acceleration performance. In addition, in the swing braking phase, the braking time of the SSEHS is about 0.6 s longer than that of the conventional swing system. This is because the maximum swing speed of SSEHS is higher than that of the conventional swing system. Meanwhile, the braking pressure of the SSEHS during energy recovery is slightly lower than the set overflow pressure to avoid energy loss caused by braking overflow.

As shown in Fig. 10, the hydraulic accumulator pressure remains consistent after each acceleration-braking working cycle of the SSEHS, indicating that the energy released and recovered by the energy storage unit is balanced. Due to the smaller designed volume of the accumulator after parameter optimization, the range in pressure of the accumulator is larger than that before parameter optimization during the

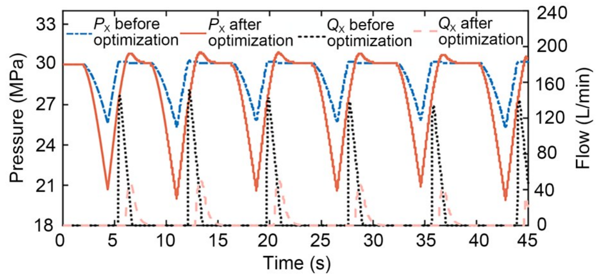

Fig. 10 Accumulator pressure (P_x) and overflow loss (Q_x) before and after parameter optimization

acceleration process, dropping from the initial 30 to 20 MPa. However, compared with the SSEHS before parameter optimization, the overflow loss of the system after parameter optimization is smaller.

4.4 Energy-saving efficiency analysis

Figs. 11–13 show the energy consumption and energy loss of different swing systems. From the data shown in Fig. 11, the output energy of the main pump in the conventional swing system is 1284.0 kJ when six slew acceleration-braking motion cycles are completed, of which the output energy in a single cycle is 214.0 kJ. For the SSEHS before parameter optimization, the output energy of the main pump is 625.6 kJ, and the output energy in a single motion cycle is 104.2 kJ. Moreover, from Fig. 11, the single-cycle

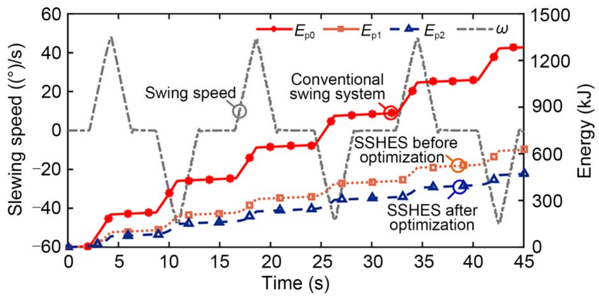

Fig. 11 Energy output of the main pumps of different systems

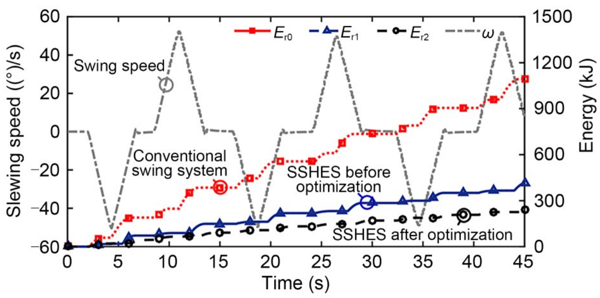

Fig. 12 Overflow energy loss of different systems

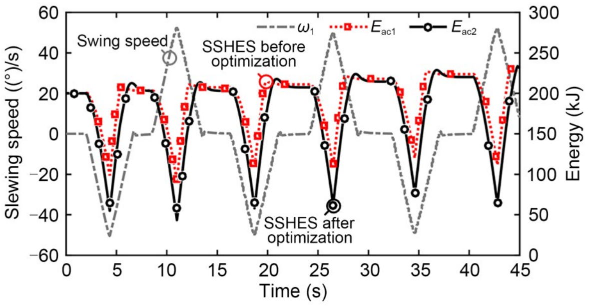

Fig. 13 Energy changes of accumulators before and after parameter optimization

output energy of the main pump in the SSEHS with optimized parameters is 78.4 kJ, which reduces the energy consumption by about 135.6 kJ compared to the conventional swing system and 25.8 kJ compared to the SSEHS without parameter optimization.

For the conventional swing system, the overflow loss during the acceleration-braking process of the slewing platform is a significant factor leading to low energy utilization. As can be seen from Fig. 12, the overflow energy loss of the conventional swing system in a single slew cycle is about 182 kJ, and the total energy loss is up to 1094 kJ for six slew motion cycles. With the help of the pressure adjustment of the HT and the energy storage unit, the total overflow loss of the swing system decreases to 416.6 kJ and further decreases to 237.7 kJ after parameter optimization. The energy change of the accumulator is shown in Fig. 13, where the initial storage energy of the accumulator is set to be the same for the convenience of comparative analysis. In a single rotation cycle, the energy change of the accumulator in the SSEHS before and after parameter optimization is 102 and 145 kJ, respectively. In contrast, the energy recovery and utilization rate of the energy storage unit after parameter optimization is higher.

5 Comparison and discussion

As shown in Figs. 8–10, in terms of the rotational dynamic performance, the proposed SSEHS can effectively reduce the pump output pressure in the acceleration process with the help of the energy storage unit while ensuring dynamic performance. The output pressure of the main pump of the optimized SSEHS is 24.4% lower than that of the SSEHS without optimization, and 57.4% lower than that of the conventional swing system. Additionally, after optimization, the overflow loss of the SSEHS is reduced, indicating that more swing braking energy is recovered by the energy storage unit, which confirms the benefits of the parameter optimization method. In terms of swing energy consumption, the proposed SSEHS achieves the recovery and reuse of swing braking energy.

As shown in Figs. 11 and 12, during a 90° rotation acceleration-braking cycle, the conventional swing system consumes 214 kJ of energy. In contrast, by recovering and reusing the swing braking energy, the slewing platform equipped with SSEHS consumes only 104 kJ. Furthermore, after optimizing the SSEHS, the slewing platform consumes only 78.4 kJ, which reduces the energy consumption by about 63.6% and 13.2% compared with the conventional swing system and the SSEHS without optimization, respectively. Meanwhile, the optimized SSEHS achieves a 78.3% reduction in overflow energy loss with the assistance of the energy storage unit. Overflow energy is often dissipated in the form of heat, and the SSEHS reduces the loss of overflow energy, which is beneficial for reducing the heat generation of the system and improving reliability.

6 Conclusions

In this study, a novel SSEHS was designed to realize energy consumption reduction of excavators with large inertia slewing platforms. An IMOPSO is proposed to optimize key parameters of the SSEHS. Based on a 50-t excavator prototype, an AMESim model with a rule-based control strategy was established. The semi-simulation and semi-experiment results showed that during a 90° rotation acceleration-braking cycle, the output pressure of the main pump in the optimized SSEHS was reduced to 11.5 MPa, while it was 14.3 MPa in the SSEHS without optimization and 27 MPa in the conventional system. Moreover, energy consumption could be reduced by about 51.4% in the SSEHS compared with the conventional swing system, and the energy-saving efficiency was improved by another 13.2% after parameter optimization. Additionally, the optimized SSEHS effectively reduced the overflow energy loss by 78.3% compared to the conventional swing system.

The designed SSEHS is also suitable for construction machinery with large inertia slewing platforms, such as rotary drilling rigs and cranes, and the proposed IMOPSO algorithm can be used for parameter matching and optimization of hydraulic hybrid systems. In future work, the optimization-based control strategy will be investigated, and the effectiveness of the proposed swing energy-saving system will be further confirmed by experiment.

Acknowledgments

This work is supported by the Changsha Major Science and Technology Plan Project, China (No. kq2207002), the Natural Science Foundation of Hunan Province (No. 2023JJ40720), and the Postgraduate Innovative Project of Central South University, China (No. 2022XQLH058).

Author contributions

Chao SHEN: methodology, software, writing, investigation, project administration. Jianxin ZHU: conceptualization, methodology, supervision. Jian CHEN and Saibai LI: data curation, validation. Lixin YI: data curation.

Conflict of interest

Chao SHEN, Jianxin ZHU, Jian CHEN, Saibai LI, and Lixin YI declare that they have no conflict of interest.

References

Abdel-baqi O, Nasiri A, Miller P, 2015. Dynamic performance improvement and peak power limiting using ultracapacitor storage system for hydraulic mining shovels. *IEEE Transactions on Industrial Electronics*, 62(5):3173-3181.
https://doi.org/10.1109/TIE.2014.2386797

Borthakur S, Subramanian SC, 2019. Design and optimization of a modified series hybrid electric vehicle powertrain. *Proceedings of the Institution of Mechanical Engineers, Part D: Journal of Automobile Engineering*, 233(6): 1419-1435.
https://doi.org/10.1177/0954407018759357

Chen QH, Lin TL, Ren HL, 2018. Parameters optimization and control strategy of power train systems in hybrid hydraulic excavators. *Mechatronics*, 56:16-25.
https://doi.org/10.1016/j.mechatronics.2018.10.003

Clerc M, Kennedy J, 2002. The particle swarm-explosion, stability, and convergence in a multidimensional complex space. *IEEE Transactions on Evolutionary Computation*, 6(1):58-73.
https://doi.org/10.1109/4235.985692

Do TC, Dang TD, Dinh TQ, et al., 2021. Developments in energy regeneration technologies for hydraulic excavators: a review. *Renewable and Sustainable Energy Reviews*, 145:111076.
https://doi.org/10.1016/j.rser.2021.111076

Gong J, Zhang DQ, Liu CS, et al., 2019a. Optimization of electro-hydraulic energy-savings in mobile machinery. *Automation in Construction*, 98:132-145.
https://doi.org/10.1016/j.autcon.2018.08.011

Gong J, Zhang DQ, Guo Y, et al., 2019b. Power control strategy and performance evaluation of a novel electro-hydraulic energy-saving system. *Applied Energy*, 233-234:724-734.
https://doi.org/10.1016/j.apenergy.2018.10.066

Gong J, Zhang DQ, Guo Y, et al., 2020. Potential energy recovery method based on alternate recovery and utilization of multiple hydraulic cylinders. *Automation in Construction*, 112:103105.
https://doi.org/10.1016/j.autcon.2020.103105

Haga M, Hiroshi W, Fujishima K, 2001. Digging control system for hydraulic excavator. *Mechatronics*, 11(6):665-676.
https://doi.org/10.1016/S0957-4158(00)00043-X

Hillman BJ, Zhang J, Tognetti LC, et al., 2016. Hydraulic Control System Having Swing Motor Energy Recovery. US Patent 9388828.

Ho TH, Ahn KK, 2012. Design and control of a closed-loop hydraulic energy-regenerative system. *Automation in Construction*, 22:444-458.
https://doi.org/10.1016/j.autcon.2011.11.004

Kwon TS, Lee SW, Sul SK, et al., 2010. Power control algorithm for hybrid excavator with supercapacitor. *IEEE Transactions on Industry Applications*, 46(4):1447-1455.
https://doi.org/10.1109/TIA.2010.2049815

Latas W, Stojek J, 2018. A new type of hydrokinetic accumulator and its simulation in hydraulic lift with energy recovery system. *Energy*, 153:836-848.
https://doi.org/10.1016/j.energy.2018.04.040

Lin TL, Liu Q, 2013. Method of parameter matching for hydraulic hybrid system for excavators. *Journal of Shanghai Jiaotong University*, 47(5):728-733 (in Chinese).
https://doi.org/10.16183/j.cnki.jsjtu.2013.05.008

Lin TL, Yang J, Liu Q, et al., 2013. Simulation study on a rotary driving system in hydraulic excavator. *Journal of Huaqiao University (Natural Science)*, 34(3):247-252 (in Chinese).
https://doi.org/10.11830/ISSN.1000-5013.2013.03.0247

Lin TL, Ye YY, Fu SJ, et al., 2014. Energy-saving system of swing for hydraulic excavators based on electric energy recovery technology. *China Journal of Highway and Transport*, 27(8):120-126 (in Chinese).
https://doi.org/10.19721/j.cnki.1001-7372.2014.08.016

Lin TL, Chen Q, Ren HL, et al., 2017. Review of boom potential energy regeneration technology for hydraulic construction machinery. *Renewable and Sustainable Energy Reviews*, 79:358-371.
https://doi.org/10.1016/j.rser.2017.05.131

Liu CS, He QH, Gong J, et al., 2016. Modeling and experimental research on rotary braking energy recovery system of hybrid excavator. *Journal of Central South University (Science and Technology)*, 47(5):1533-1542 (in Chinese).
https://doi.org/10.11817/j.issn.1672-7207.2016.05.012

Poli R, Kennedy J, Blackwell T, 2007. Particle swarm optimization: an overview. *Swarm Intelligence*, 1(1):33-57.
https://doi.org/10.1007/s11721-007-0002-0

Prasanthi A, Shareef H, Asna M, et al., 2021. Optimization of hybrid energy systems and adaptive energy management for hybrid electric vehicles. *Energy Conversion and Management*, 243:114357.
https://doi.org/10.1016/j.enconman.2021.114357

Qu SY, Fassbender D, Vacca A, et al., 2021. A high-efficient solution for electro-hydraulic actuators with energy regeneration capability. *Energy*, 216:119291.
https://doi.org/10.1016/j.energy.2020.119291

Shang TL, Zhang J, Ma PF, 2014. Hydraulic Control System Having Energy Recovery. US Patent 8726645.

Suppapitnarm A, Seffen KA, Parks GT, et al., 2000. A simulated annealing algorithm for multi-objective optimization. *Engineering Optimization*, 33(1):59-85.
https://doi.org/10.1080/03052150008940911

Thompson B, Yoon HS, Kim J, et al., 2014. Swing Energy Recuperation Scheme for Hydraulic Excavators. SAE Technical Paper No. 2014-01-2402, SAE International, Warrendale, USA.
https://doi.org/10.4271/2014-01-2402

Tong ZM, Wu SS, Tong SG, et al., 2020. Energy-saving technologies for construction machinery: a review of electro-hydraulic pump-valve coordinated system. *Journal of Zhejiang University-SCIENCE A (Applied Physics & Engineering)*, 21(5):331-349.
https://doi.org/10.1631/jzus.A2000094

Tong ZM, Miao JZ, Li YS, et al., 2021. Development of electric construction machinery in China: a review of key technologies and future directions. *Journal of Zhejiang University-SCIENCE A (Applied Physics & Engineering)*, 22(4):245-264.
https://doi.org/10.1631/jzus.A2100006

Wang HM, Wang QF, 2020. Parameter matching and control of series hybrid hydraulic excavator based on electro-hydraulic composite energy storage. *IEEE Access*, 8:111899-111912.
https://doi.org/10.1109/ACCESS.2020.2999620

Wang HM, Wang QF, Hu BZ, 2017. A review of developments in energy storage systems for hybrid excavators. *Automation in Construction*, 80:1-10.
https://doi.org/10.1016/j.autcon.2017.03.010

Wei LX, Ning ZQ, Quan L, et al., 2022. Research on parameter matching of the asymmetric pump potential energy recovery system based on multi-core parallel optimization method. *Processes*, 10(11):2298.
https://doi.org/10.3390/pr10112298

Xia LP, Quan L, Ge L, et al., 2018. Energy efficiency analysis of integrated drive and energy recuperation system for hydraulic excavator boom. *Energy Conversion and Management*, 156:680-687.
https://doi.org/10.1016/j.enconman.2017.11.074

Yu YX, Ahn KK, 2020a. Improvement of energy regeneration for hydraulic excavator swing system. *International Journal of Precision Engineering and Manufacturing-Green Technology*, 7(1):53-67.
https://doi.org/10.1007/s40684-019-00165-7

Yu YX, Ahn KK, 2020b. Energy regeneration and reuse of excavator swing system with hydraulic accumulator. *International Journal of Precision Engineering and Manufacturing-Green Technology*, 7(4):859-873.
https://doi.org/10.1007/s40684-019-00157-7

Electronic supplementary materials

Section S1